TA ed.

APPLICATION OF MOMENT REALIZABILITY CRITERIA FOR COUPLING OF THE BOLTZMANN AND EULER EQUATIONS

Sudarshan Tiwari

Fachbereich Mathematik
Universität Kaiserslautern
67663 Kaiserslautern
Germany

ABSTRACT

The moment realizability criteria have been used to test the domains of validity of the Boltzmann and Euler equations. With the help of this criteria the coupling of the Boltzmann and Euler equations have been performed in two dimensional spatial space. The time evolution of domain decompositions for such equations have been presented in different time steps. The numerical results obtained from the coupling code have been compared with those from the pure Boltzmann one.

1 INTRODUCTION

In the simulation of the rarefied gas flows different mean free paths (average distance travelled between collisions) characterize the different mathematical problems. If the mean free path is much less than the characteristic length of the flow so that the gas is sufficiently dense, fluid dynamic equations give the description of the flows. In the rarefied case, the mean free path is not much smaller than the characteristic length, hence the description of the flow can be obtained from the Boltzmann equation.

The most widely used simulation methods for the Boltzmann equation are the particle methods like Direct Simulation Monte Carlo Methods (DSMC) [3] and Finite Pointset Method (FPM) [1], [2], [15], [17]. Since the grid size which is used in the particle methods should be of the order of the mean free path, the computational efforts for the Boltzmann equation become high as the mean free path tends to zero. From the classical theory, as the mean free

path tends to zero, the Boltzmann equation can be approximated by the fluid dynamic equations (Euler or Navier-Stokes) [7].

But these limiting equations may not be valid everywhere. Therefore, one may solve the Boltzmann equation only where it is necessary and fluid dynamic equations wherever possible. For this purpose, one needs a criterion which detects the domains of validity for the Boltzmann and fluid dynamic equations. Some criteria for the domains of validity for the Boltzmann and Euler equations have been proposed in [18], [19].

In this paper we present the moment realizability criteria, proposed by Levermore *et al* [13]. The authors in [13] have basically used this criteria for the validity of the Navier-Stokes approximation. In our case the same is used for the domains of validity for the Euler equations. The criteria is based on the deviation of an $(m \times m)$- validity matrix from its equilibrium value.

For the past few years several attempts have been made to couple the Boltzmann and fluid dynamic equations. We refer to [4], [5], [12], [14], [16], [18], [19], [20] for the coupling of the Boltzmann and fluid dynamic equations.

We organize this paper as follows. In section 2 we present the equations to be coupled and their numerical solvers. In section 3, the derivation of the moment realizability criteria is given. Finally, some numerical results are presented in section 4.

2 EQUATIONS TO BE COUPLED AND THEIR SOLVERS

2.1 The Boltzmann Equation

We consider the perfect monoatomic gas. The Boltzmann equation is the time evolution of the distribution function $f(t, x, v)$ for the particles of velocity $v \in \mathbb{R}^3$, at point $x \in \Omega \subset \mathbb{R}^d (d = 1, 2, 3)$ at a time $t \in \mathbb{R}_+$ and is given by

$$\frac{\partial f}{\partial t} + v.\nabla_x f = \frac{1}{\epsilon} J(f, f), \tag{1}$$

with

$$J(f, f) = \int_{\mathbb{R}^3} \int_{S^2} k(|v - w|, \eta)[f(v')f(w') - f(v)f(w)]d\omega(\eta)dw \tag{2}$$

$$v^{'} = T_{v,w}(\eta) = v - \eta < \eta, v - w >,\ w^{'} = T_{w,v}(\eta) \tag{3}$$

and ϵ is proportional to the mean free path. On the right hand side of (2) the function $k(|v-w|,\eta)$ is called the collision kernel, which depends on the interaction potential. In this paper the hard sphere model has been considered. For more details about the Boltzmann equation we refer to [7]. We solve (1) with the initial condition

$$f(0,x,v) = f_0(x,v) \tag{4}$$

and some boundary conditions, described in section 4.2.

We state the following important properties of the Boltzmann equation

(a) Mass, momentum and energy of particles are conserved by the collision process

$$\int_{\mathbb{R}^3} \psi_\alpha J(f,f)dv = 0,\ \alpha = 0,1,2,3,4, \tag{5}$$

where $\psi_0 = 1, \psi_i = v_i, i = 1,2,3$ and $\psi_4 = |v|^2$, called collision invariants.

(b) As ϵ tends to 0 one can prove [6] that the Boltzmann distribution function f tends to a local Maxwellian

$$f_M := f_M[\rho,u,T](t,x) = \frac{\rho}{(2\pi RT)^{3/2}}\, e^{-\frac{|v-u|^2}{2RT}}, \tag{6}$$

where R is the gas constant and the parameters $\rho(t,x),\ u(t,x),\ T(t,x)$ approximate the compressible Euler equations.

2.2 The Compressible Euler Equations

The quantities of interest are the macroscopic ones given by the following moments:

$$\rho(t,x) = \int_{\mathbb{R}^3} f(t,x,v)dv \qquad \text{(density)} \tag{7}$$

$$u(t,x) = \frac{1}{\rho}\int_{\mathbb{R}^3} v f(t,x,v)dv \qquad \text{(mean velocity)} \tag{8}$$

$$E(t,x) = \frac{1}{\rho}\int_{\mathbb{R}^3} \frac{|v|^2}{2} f(t,x,v)dv \qquad \text{(specific energy)} \tag{9}$$

$$\tau_{ij} = \int_{\mathbb{R}^3} (v_i - u_i)(v_j - u_j) f(t,x,v)dv - p\delta_{ij} \qquad \text{(stress tensor)}, \tag{10}$$

where p is the static pressure and δ_{ij} the Kronecker symbol and

$$q_j = \frac{1}{2}\int_{\mathbb{R}^3}(v_j - u_j)|v-u|^2 f(t,x,v)dv \qquad \text{(heat flux)}. \tag{11}$$

Multiplying the Boltzmann equation (1) by the collision invariants $1, v, |v|^2/2$ and then integrating with respect to v over $\mathbb{R}^3$, one gets the following system of conservation equations

$$\frac{\partial \rho}{\partial t} + \sum_{j=1}^{3}\frac{\partial}{\partial x_j}(\rho u_j) = 0 \tag{12}$$

$$\frac{\partial}{\partial t}(\rho u_i) + \sum_{j=1}^{3}\frac{\partial}{\partial x_j}(\rho u_i u_j + p\delta_{ij}) = \sum_{j=1}^{3}\frac{\partial}{\partial x_j}(\tau_{ij}) \tag{13}$$

$$\frac{\partial}{\partial t}(\rho E) + \sum_{j=1}^{3}\frac{\partial}{\partial x_j}(\rho \dot{E} u_j + p u_j) = \sum_{j=1}^{3}\frac{\partial}{\partial x_j}(q_j + \sum_{i=1}^{3} u_i \tau_{ij}). \tag{14}$$

This system has more unknowns than equations. Therefore, this is not a closed system. Suppose $f = f_M$, then $\tau_{ij} = 0$ and $q_j = 0$ by symmetry and the following relations hold:

$$p = \int_{\mathbb{R}^3}(v_i - u_i)^2 f_M dv = \rho RT, \; E = \frac{3}{2}RT + \frac{|u|^2}{2}. \tag{15}$$

Then the above system of equations reduces to the compressible Euler equations. These equations have to be solved with suitable initial and boundary conditions.

2.3 The Boltzmann Solver

We solve the Boltzmann equation by the particle method or more specifically, finite pointset method. For details about this method we refer to [15], [17]. The particle method for the Boltzmann equation is based on the time splitting of the equation. Let $T > 0$ be a given time and $m \in \mathbb{N}$. Then one takes the discrete time steps $t_k = k \cdot \Delta t$, where $\Delta t = T/m$. For each time interval $[t_k, t_{k+1})$ we consider the following two equations:

1. The free transport equation

$$\frac{\partial g}{\partial t} + v \cdot \nabla_x g = 0 \tag{16}$$

with initial condition

$$g(t_k) = f(t_k) \tag{17}$$

and some boundary conditions as described later.

2. The collision

$$\frac{\partial \tilde{f}}{\partial t} = \frac{1}{\epsilon} J(\tilde{f}, \tilde{f}) \tag{18}$$

with initial condition

$$\tilde{f}(t_k) = g(t_{k+1}) \tag{19}$$

and $f(t_{k+1}) = \tilde{f}(t_{k+1})$ being a solution of (1) at time t_{k+1}.

The particle simulation of (16) is based on the approximation of the initial density $f_k(x, v)$ by a discrete measure (a sum of Dirac masses)

$$f_k(x, v) \approx \sum_{j=1}^{N} \alpha_j \delta(x - x_j(t_k)) \delta(v - v_j(t_k)). \tag{20}$$

The positions $x_i(t_k)$ of the particles change (during the free flow only) as per the following relation

$$x_j(t_k + \Delta t) = x_j(t_k) + \Delta t \cdot v_j(t_k), \tag{21}$$

where the velocities change during the collision step. In our simulation we have considered all the particles of equal weight $1/N$.

For the simulation of equation (18) one has to introduce a spatial mollifier since the collision integral $J(f, f)$ is a local operator in space and time. We divide the computational domain into many regular cells C where the density $f(t, x, v)$ is substituted by $f_C(t, v)$ for $x \in C$ and

$$f_C(t, v) = \frac{1}{\text{Vol}(C)} \int_C f(t, y, v) dy. \tag{22}$$

Now, it is sufficient to describe the particle simulation of the following space homogeneous Boltzmann equation

$$\frac{\partial f}{\partial t} = \frac{1}{\epsilon} J(f, f) \tag{23}$$

with an initial condition

$$f(0, v) = f_0(v). \tag{24}$$

Discretizing the equation (23) with respect to time and using an Euler step, one gets

$$\begin{aligned} f(\Delta t, v) = & \left(1 - \frac{\Delta t}{\epsilon} \int_{\mathbb{R}^3} \int_{S^2_+} k(|v - w|, \eta) f_0(w) d\omega(\eta) dw \right) f_0(v) \\ & + \frac{\Delta t}{\epsilon} \int_{\mathbb{R}^3} \int_{S^2_+} k(|v - w|, \eta) f_0(v') f_0(w') d\omega(\eta) dw. \end{aligned} \tag{25}$$

Since the approximation of the function f is based on the weak convergence of measures, it is useful to consider (25) in a weak formulation

$$\int_{\mathbb{R}^3} \phi(v) f(\Delta t, v) dv =$$
$$\int_{\mathbb{R}^3} \left[1 - \frac{\Delta t}{\epsilon} \int_{\mathbb{R}^3} \int_{S^2_+} k(|v-w|, \eta) f_0(w) d\omega(\eta) dw \right] \phi(v) f_0(v) dv$$
$$+ \frac{\Delta t}{\epsilon} \int_{\mathbb{R}^3} \int_{\mathbb{R}^3} \int_{S^2_+} k(|v-w|, \eta) \phi(v) f_0(v') f_0(w') d\omega(\eta) dv dw \qquad (26)$$

for all $\phi \in C^b$, set of all bounded and continuous functions in $\mathbb{R}^3$. Assuming $\|f\|_1 = 1$ and the collision transformations (3) imply that $dv'dw' = dvdw$, $|v' - w'| = |v - w|$ one gets

$$\int_{\mathbb{R}^3} \phi(v) f(\Delta t, v) dv = \int_{\mathbb{R}^3} \int_{\mathbb{R}^3} (R\phi)(v, w) f_0(v) f_0(w) dv dw \qquad (27)$$

where

$$(R\phi)(v, w) = \left[1 - \frac{\Delta t}{\epsilon} \int_{S^2_+} k(|v-w|, \eta) d\omega(\eta) \right] \phi(v)$$
$$+ \frac{\Delta t}{\epsilon} \int_{S^2_+} k(|v-w|, \eta) \phi(v') d\omega(\eta).$$

To solve equation (27) we need an approximation of the product measure

$$d\omega(\eta) f(0, v) f(0, w) dw dv$$

by some $\sum_{j=1}^N \alpha_j' \delta_{(\eta_j, v_j, w_j)}$, given only an approximation $\sum_{j=1}^N \alpha_j \delta_{v_j}$ of $f(0, v)dv$. If this problem is solved and $\sum_{j=1}^N \alpha_j' \delta_{(\eta_j, v_j, w_j)}$ is determined, one can compute the time evolution of the measure due to (27). The factor $1 - \frac{\Delta t}{\epsilon} k$ is interpreted as a probability for a dummy collision, keeping the old velocities. $\frac{\Delta t}{\epsilon} k$ is the probability for a real collision, changing $v_j \to v_j' = T_{v_j, w_j}(\eta_j)$. For more details about the solution procedure for the space homogeneous Boltzmann equation we refer to [2], [15], [17].

One observes that, to guarantee the positivity of the function $f(\Delta t, v)$, we need the following restriction on the time step

$$1 - \frac{\Delta t}{\epsilon} k \geq 0. \qquad (28)$$

This means that for $\epsilon \to 0$ the time step Δt has to be shrank with ϵ, the equations are becoming stiff. The method becomes exceedingly expensive for small Knudsen numbers.

2.4 The Euler Solver

We solve the Euler equations also by the particle method based on the kinetic scheme. Earlier workers [8], [9], [10], [11], have reported this scheme in detail. It is the direct consequence of the solution scheme for the Boltzmann equation. It also consists of two steps as in the case of the Boltzmann equation:

1. The free transport equation:

$$\frac{\partial f}{\partial t} + v \cdot \nabla_x f = 0. \tag{29}$$

2. The relaxation:

$$J(f, f) = 0. \tag{30}$$

The equation (30) is a relaxation to a thermodynamic equilibrium, whose solution is a local Maxwellian. As in the Boltzmann case we repeat above procedure until we reach the required time.

In the relaxation step, we reproduce the particles according to a simple function f_K, introduced by Kaniel [11], since it is computationally faster than that of f_M and also because the results obtained are found to be good. For a monoatomic gas it is given by

$$f_K = \begin{cases} \dfrac{3}{4\pi}\dfrac{\rho}{(5RT)^{3/2}} & : \ |v-u| \leq \sqrt{5RT} \\ 0 & : \ |v-u| > \sqrt{5RT} \end{cases} . \tag{31}$$

2.5 The Boundary Conditions

During the free flow we take the boundary conditions into account. In this step the particles may hit the spatial boundary, leave the domain or enter it. One has to take care of the corresponding boundary conditions.

- Particle may leave the computational domain (absorption), for example, on the boundaries as denoted by Γ_2 in Figure 1.
- Particles may enter the spatial domain at parts of the boundary. On the left boundary as indicated by Γ_1 in Figure 1 we consider a layer of boundary cells. At each time step and in each boundary cell we generate N particles randomly with a uniform distribution and a Maxwellian distribution in the physical and the velocity spaces, respectively.

- Particles may be re-emitted at a physical boundary (gas surface interaction). On the boundary Γ_3 in Figure 1 we use a diffuse reflection with a complete thermal accommodation [7]. In other words, each particle colliding with the wall is re-emitted with the velocity distribution of the form $v' = v'_d$ where v'_d is the velocity of the particle re-emitted with a Maxwellian distribution at a wall temperature T_W. Let (t, n, z) be a local orthonormal basis, with n normal to the wall, then, we have

$$v'_{d_t} = \sqrt{-RT_W \ln \alpha_1} \cos 2\pi\alpha_2 \tag{32}$$

$$v'_{d_z} = \sqrt{-RT_W \ln \alpha_1} \sin 2\pi\alpha_2 \tag{33}$$

$$v'_{d_n} = \sqrt{-RT_W \ln \alpha_3}, \tag{34}$$

where α_1, α_2, α_3 are the uniformly distributed random numbers between 0 and 1.

2.6 The Coupling Algorithm

1. Approximate the initial distribution function by the Dirac masses.

2. For time step 1 to K:

   - Generate the particles having a Maxwellian distribution in the velocity space and a uniform distribution in the physical one at the boundary cells.

   - Advance the particles in a free flow

$$x_j(t + \Delta t) = x_j(t) + \Delta t \cdot v_j(t).$$

   - If the particle collide with the surface boundary, reflect it according to the above described boundary condition and continue the free flow with a new velocity until Δt is over.

   - Erase the particles that leave the domain.

3. Check whether the cells are either Euler or Boltzmann cells using the criteria, described in the next section.

4a. Consider intermolecular collisions in the Boltzmann cells.

4b. Project the distribution function into a local thermal equilibrium in the Euler cells.

5. Go to step 2.

3 MOMENT REALIZABILITY CRITERIA

The moment realizability criteria is proposed by Levermore *et al* [13]. We give a brief description of moment realizability criteria. If the distribution function f is nonnegative, the same is true for the quantity $\int \psi^2 f dv$ for any function $\psi = \psi(v)$. Let ψ be an arbitrary polynomial spanned by a general set of polynomials in the components of v. More, precisely, let $c = c(v)$ denotes a column vector of m given polynomials then for $\psi = a^t c$ for an arbitrary $a \in \mathbb{R}^m$, where a^t denotes the transpose of the vector a, we have

$$a^t(\int_{\mathbb{R}^3} cc^t f dv)a = \int_{\mathbb{R}^3} (a^t c)^2 f dv \quad \geq 0, \quad \text{for every} \quad a \in \mathbb{R}^m. \tag{35}$$

If f is nonnegative and not identically zero a. e., then, for every c the $(m \times m)$-matrix

$$M = \frac{1}{\rho} \int_{\mathbb{R}^3} cc^t f dv \tag{36}$$

is positive semi-definite.

We choose the vector c which includes all the necessary densities and fluxes of the local conservation laws (12)- (14)

$$c = \left(1, \frac{v-u}{(RT)^{1/2}}, (\frac{2}{5})^{1/2}(\frac{|v-u|^2}{2RT} - \frac{5}{2})\right)^t. \tag{37}$$

The components of c are orthonormal to $\frac{1}{\rho} f_M$. This choice of c corresponds to the (5×5)-symmetric matrix

$$M = \begin{pmatrix} 1 & 0 & 0 \\ 0 & I + A & \sqrt{\frac{2}{5}} B \\ 0 & \sqrt{\frac{2}{5}} B^t & L \end{pmatrix}, \tag{38}$$

where

$$A = \frac{1}{\rho RT} \int_{\mathbb{R}^3} (v-u)\,(v-u)^t f dv - I \tag{39}$$

$$B = \frac{1}{\rho} \int_{\mathbb{R}^3} \left(\frac{|v-u|^2}{2RT} - \frac{5}{2}\right) \frac{v-u}{\sqrt{RT}} f dv \tag{40}$$

$$L = \frac{1}{\rho}\frac{2}{5} \int_{\mathbb{R}^3} \left(\frac{|v-u|^2}{2RT} - \frac{5}{2}\right)^2 f dv = \frac{1}{10\rho(RT)^2} \int_{\mathbb{R}^3} |v-u|^4 f dv - \frac{1}{2}. \tag{41}$$

If $f = f_M$, then, $L = 1$, A is a zero matrix and B a zero vector so that the matrix $M = I$, the equilibrium matrix and has the eigenvalues equal to 1. When f has a deviation from an equilibrium or a Maxwellian, the corresponding matrix M also has the same from the identity matrix. Equivalently, the eigenvalues have deviation from their equilibrium values 1. A large deviation of f from f_M indicates that of M from the identity matrix I.

Since the distribution function f is nonnegative, the approximation to it need not be the same. The components of the matrix M are the moments of the nonnegative distribution function f and the matrix is positive semi-definite, equivalently, its eigenvalues are nonnegative. If we compute the components of the matrix M as the moments of an approximated distribution function of f, the matrix can be negative semi-definite.

We realize this situation by the following considerations. The fluid dynamic description is valid if the distribution function is close enough to a local Maxwellian. We assume that the distribution function f has a small deviation from a local Maxwellian. Then, we approximate it by

$$f = f_M(1 + \phi), \tag{42}$$

where ϕf_M denotes the perturbation of f from f_M. Since the first five moments (7)-(9) of f are those of f_M. Then, we have

$$\int_{\mathbb{R}^3} \phi f_M dv = 0 \tag{43}$$

$$\int_{\mathbb{R}^3} v\phi f_M dv = 0 \tag{44}$$

$$\int_{\mathbb{R}^3} |v|^2 \phi f_M dv = 0. \tag{45}$$

Furthermore, from (10) and (11), we have

$$\int_{\mathbb{R}^3} (v-u)(v-u)^t \phi f_M dv = \tau. \tag{46}$$

$$\frac{1}{2}\int_{\mathbb{R}^3} (v-u)|v-u|^2 \phi f_M dv = q \tag{47}$$

With the help of the above thirteen equations (43)- (47) we express ϕ as a polynomial

$$\phi = a + \langle b, v-u\rangle + (v-u)^t S(v-u) + \langle d, v-u\rangle |v-u|^2, \tag{48}$$

where a is a scalar, b, d are vectors in $\mathbb{R}^3$ and S is a (3×3)-symmetric matrix.

One can determine all the coefficients of the polynomial (48) by substituting ϕ in equations (43)- (47) and gets

$$\phi = \frac{\langle v-u, q\rangle}{\rho(RT)^2}\left[\frac{|v-u|^2}{5RT} - 1\right] + \frac{1}{2\rho(RT)^2}(v-u)^t\tau(v-u). \tag{49}$$

Our main interest is to find the region where the above approximation $f = f_M(1+\phi)$ cannot be realized. That is, find the region where the above approximation (42) of f is not valid. It can be even negative, which gives the failure of the fluid dynamic description. In such regions f may have large deviation from f_M. This deviation can be monitored during the simulation by checking the deviation of the matrix M from the identity matrix I.

The calculation will be simpler if we use some transformation of the matrix M. Assuming $L > 0$ and defining the matrix

$$Q = \begin{pmatrix} 1 & 0 & 0 \\ 0 & I & 0 \\ 0 & -\sqrt{\frac{2}{5}}\frac{B^t}{L} & 1 \end{pmatrix}, \tag{50}$$

it follows that

$$Q^tMQ = \begin{pmatrix} 1 & 0 & 0 \\ 0 & I + A - \frac{2BB^t}{5L} & 0 \\ 0 & 0 & L \end{pmatrix}. \tag{51}$$

Hence, when $L > 0$, the positive semi-definiteness of the matrix M is equivalent to the positive semi-definiteness of the following (3×3)-matrix

$$V = I + A - \frac{2BB^t}{5L}. \tag{52}$$

As a criterion for an equilibrium, the negativity as well as the deviation of the eigenvalues of V from the equilibrium values 1 give the region of breaking the fluid dynamic description.

Now, we compute the components A, B and L of the matrices for $f = f_M(1+\phi)$. Firstly, consider

$$\begin{aligned} A = \frac{1}{\rho}\int_{\mathbb{R}^3} Af dv &= \frac{1}{\rho}\int_{\mathbb{R}^3} Af_M dv + \frac{1}{\rho}\int_{\mathbb{R}^3} A\phi f_M dv \\ &= \frac{1}{\rho}\int_{\mathbb{R}^3} (v-u)\,(v-u)^t\phi f_M dv = \frac{\tau}{\rho RT}. \end{aligned} \tag{53}$$

Next,

$$\begin{aligned} B &= \frac{1}{\rho}\int_{\mathbb{R}^3}\left(\frac{|v-u|^2}{2RT}-\frac{5}{2}\right)\frac{v-u}{\sqrt{RT}}f_M dv+\frac{1}{\rho}\int_{\mathbb{R}^3}\left(\frac{|v-u|^2}{2RT}-\frac{5}{2}\right)\frac{v-u}{\sqrt{RT}}\phi f_M dv \\ &= \frac{q}{\rho(RT)^{3/2}}. \end{aligned} \tag{54}$$

Finally,

$$\begin{aligned} L &= \frac{1}{10\rho(RT)^{3/2}}\int_{\mathbb{R}^3}|v-u|^4 f dv-\frac{1}{2} \\ &= \frac{1}{10\rho(RT)^{3/2}}\int_{\mathbb{R}^3}|v-u|^4 f_M dv-\frac{1}{2}+\frac{1}{10\rho(RT)^{3/2}}\int_{\mathbb{R}^3}|v-u|^4\phi f_M dv. \end{aligned}$$

Since $\frac{1}{10\rho(RT)^{3/2}}\int_{\mathbb{R}^3}|v-u|^4 f_M dv-\frac{1}{2}=1$, we have

$$L=1+\frac{1}{10\rho(RT)^{3/2}}\int_{\mathbb{R}^3}|v-u|^4\phi f_M dv. \tag{55}$$

Now we compute the right hand side of the integral (55) for given ϕ from (49). Then

$$\begin{aligned} \int_{\mathbb{R}^3}|v-u|^4\phi f_M dv &= \frac{1}{(RT)^{3/2}}\int_{\mathbb{R}^3}|v-u|^4\langle v-u,q\rangle\left(\frac{|v-u|^2}{2RT}-1\right)f_M dv \\ &+ \frac{1}{2\rho(RT)^{3/2}}\int_{\mathbb{R}^3}|v-u|^4(v-u)^t\tau(v-u)f_M dv. \end{aligned}$$

Since first integral vanishes because of the symmetry of the Maxwellian f_M, we have

$$\int_{\mathbb{R}^3}|v-u|^4\phi f_M dv=\frac{1}{(RT)^{3/2}}\int_{\mathbb{R}^3}|v-u|^4(v-u)^T\tau(v-u)e^{-\frac{|v-u|^2}{2RT}}dv$$

$$=\int_{\mathbb{R}^3}|v-u|^4\left[\sum_{i=1}^{3}\tau_{ii}(v_i-u_i)^2+2\sum_{i\neq j}\tau_{ij}(v_i-u_i)(v_j-u_j)\right]e^{-\frac{|v-u|^2}{2RT}}dv.$$

Transforming the vector $v-u$ in spherical coordinates and by simple calculation we get

$$\begin{aligned} \int_{\mathbb{R}^3}|v-u|^4(v_1-u_1)^2e^{-\frac{|v-u|^2}{2RT}} &= \int_{\mathbb{R}^3}|v-u|^4(v_1-u_1)^2e^{-\frac{|v-u|^2}{2RT}} \\ &= \int_{\mathbb{R}^3}|v-u|^4(v_1-u_1)^2e^{-\frac{|v-u|^2}{2RT}} \\ &= 70\pi(RT)^4(2RT)^{1/2}. \end{aligned}$$

Similarly,

$$\int_{\mathbb{R}^3} |v-u|^4 (v_2-u_2)^2 e^{-\frac{|v-u|^2}{2RT}} = \int_{\mathbb{R}^3} |v-u|^4 (v_3-u_3)^2 e^{-\frac{|v-u|^2}{2RT}} = 70\pi (RT)^4 (2RT)^{1/2}.$$

And

$$\begin{aligned} \int_{\mathbb{R}^3} |v-u|^4 (v_1-u_1)(v_2-u_2) e^{-\frac{|v-u|^2}{2RT}} &= \int_{\mathbb{R}^3} |v-u|^4 (v_2-u_2)(v_3-u_3) e^{-\frac{|v-u|^2}{2RT}} \\ &= \int_{\mathbb{R}^3} |v-u|^4 (v_1-u_1)(v_3-u_3) e^{-\frac{|v-u|^2}{2RT}} \\ &= 0. \end{aligned}$$

This implies

$$\int_{\mathbb{R}^3} |v-u|^4 \phi f_M dv = 70\pi (RT)^4 (2RT)^{1/2} (\tau_{11}+\tau_{22}+\tau_{33}) = 0, \tag{56}$$

since $\tau_{11}+\tau_{22}+\tau_{33}=0$.

Form (55) and (56) we have $L=1$ for $f=f_M(1+\phi)$. Hence, it is enough to check the positive semi-definiteness of the (3×3)-matrix

$$V = I + A - \frac{2BB^t}{5}. \tag{57}$$

We may also consider the matrix V in (57) as a perturbation of the identity matrix I. All choices of the vector $c(v)$ whose elements span the space of polynomials in v correspond to the moment realizability criteria defined by the positive semi-definiteness of the matrix M. In fact, any operation which does not change the sign of the eigenvalues of the matrix M may be performed without changing the criterion. This includes change of basis operations such as (50).

More general criteria for assessing the validity of fluid dynamic equations are suggested by the form of the matrix M in (38). Because the vector c in (37) was chosen to have orthonormal element with respect to integration against the Maxwellian equilibrium distribution f_M/ρ, it follows that at equilibrium the matrix M must be the identity matrix. For the distribution, perturbed from a Maxwellian, one can view M as a perturbation of the identity matrix. Large deviation of M from I indicate the same from a equilibrium. The moment realizability criterion states that the fluid dynamic description has broken down when the perturbation is too large that M is no longer positive semi-definite.

Since the matrix Q in (50) is not orthonormal, the matrices V and M will not share the same eigenvalues. Thus assessing breakdown with V requires a different tuning than M. Since V is smaller and simpler, the use of the matrix V could be enough as criteria of equilibrium.

For $f = f_M(1+\phi)$, the matrix (38) is given by

$$M_1 = \begin{pmatrix} 1 & 0 & 0 \\ 0 & I+A & \sqrt{\frac{2}{5}}B \\ 0 & \sqrt{\frac{2}{5}}B^T & 1 \end{pmatrix}. \tag{58}$$

In the next section we compute the eigenvalues of both matrices V and M_1. With the help of their eigenvalues, we justify the domains of validity for the Boltzmann and Euler equations.

4 NUMERICAL RESULTS

We consider a two dimensional flow of a perfect monoatomic gas flowing at hypersonic speed around an ellipse with major and minor axes $1.0m$ and $0.5m$ respectively. The computational domain Ω is a rectangle with size $6m \times 4m$ as shown in Figure 1.

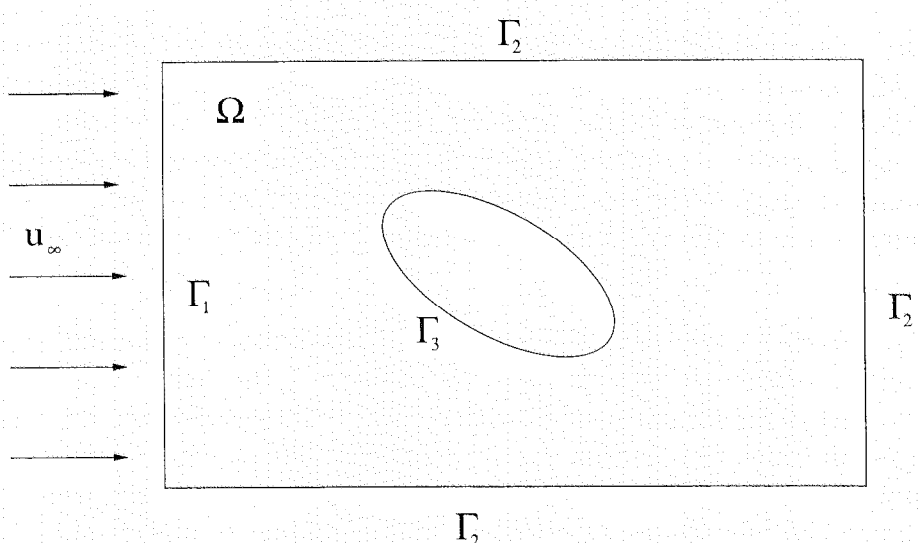

Figure 1: Computational domain

As the initial condition we use the following Maxwellian distribution

$$f(0,x,v) = \frac{\rho_\infty}{(2\pi RT_\infty)^{3/2}}\, e^{-\frac{|v-u_\infty|^2}{2RT_\infty}} \tag{59}$$

and the boundary conditions as described above.

We divide the computational domain Ω into many rectangular cells of the size of the global mean free path, that is, $dx = \lambda$. We choose the time step $\Delta t = dx/u_\infty$ and compute until the steady state is reached. A total of 400 time steps were taken. In the simulation the following parameters are considered: $\lambda = 0.1m$, Mach number = 15, $T_\infty = 200K$, gas constant $R = 208Jkg/K$, $T_W = 1000K$, angle of attack = 30^0, the number of particles per cell at the beginning = 50.

We first compute the eigenvalues of the matrix M_1. In Figure 2 we have plotted, in a steady state, the four eigenvalues of the matrix M_1 on the middle row of the computational domain since one of them is identically equal to one.

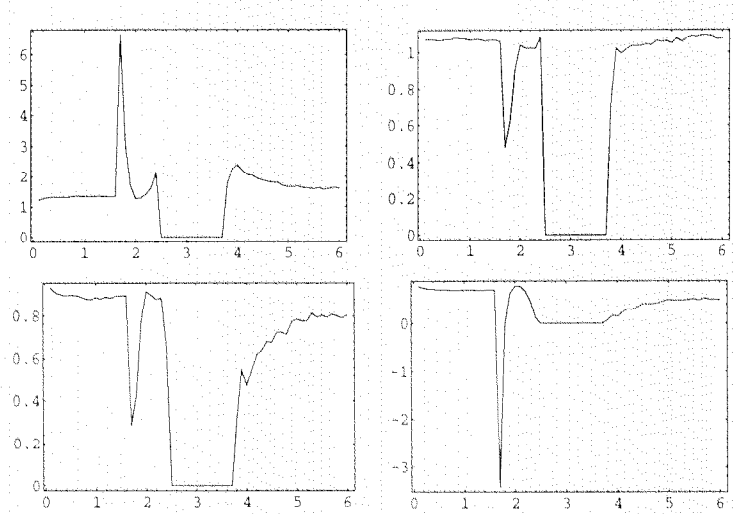

Figure 2: The four eigenvalues of the matrix M

In Figure 2 we see that one eigenvalue is negative in the shock region. This shows that the approximation of f as a small deviation from a local Maxwellian is extremely bad in a such region. The other eigenvalues are positive but have significant deviation from the unity in non-equilibrium regions.

A choice of a particular eigenvalue may not give the general criterion for an equilibrium. Therefore, for general criteria we consider the invariants of the matrix, which contain all the eigenvalues. Let $\lambda_1, \lambda_2, \lambda_3, \lambda_4$ be eigenvalues of the matrix M_1. If the distribution function f is close enough to the Maxwellian f_M, these all eigenvalues are equal to the equilibrium values 1. Therefore, if the particle distribution is close enough to a Maxwellian, the invariants of the matrix M_1 must satisfy the following relations:

$$\frac{1}{4}(\lambda_1 + \lambda_2 + \lambda_3 + \lambda_4) = 1 \tag{60}$$

$$\frac{1}{6}(\lambda_1\lambda_2 + \lambda_1\lambda_3 + \lambda_1\lambda_4 + \lambda_2\lambda_3 + \lambda_2\lambda_4 + \lambda_3\lambda_4) = 1 \tag{61}$$

$$\frac{1}{4}(\lambda_1\lambda_2\lambda_3 + \lambda_1\lambda_2\lambda_4 + \lambda_1\lambda_3\lambda_4 + \lambda_2\lambda_3\lambda_4) = 1 \tag{62}$$

$$\lambda_1 \cdot \lambda_2 \cdot \lambda_3 \cdot \lambda_4 = 1. \tag{63}$$

In Figure 3 the four invariants (60)- (63) are plotted on the middle row of the computational domain.

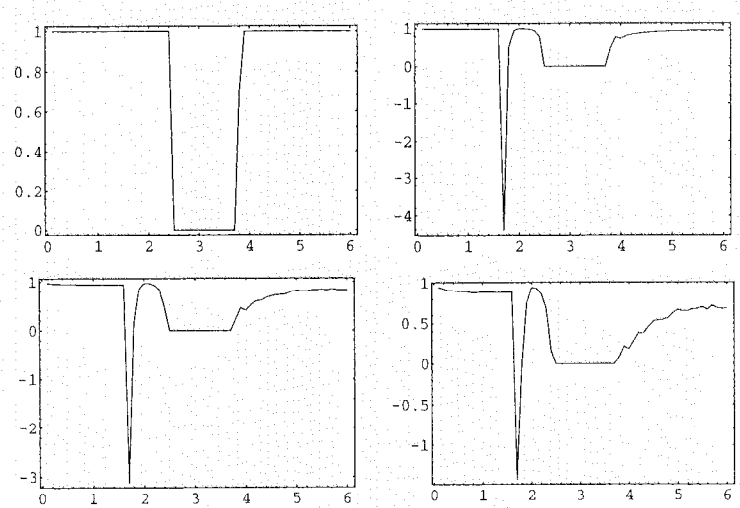

Figure 3: The four invariants of the matrix M

As a criterion for a local thermal equilibrium we consider the invariant (61). We assume that if this normalized invariant lies between 0.8 and 1.2, then, the cells are Euler ones, otherwise they are Boltzmann ones. In Figure 4 we have

plotted the domain decompositions for the Boltzmann and Euler equations in the time steps $10, 25, 50, 100$.

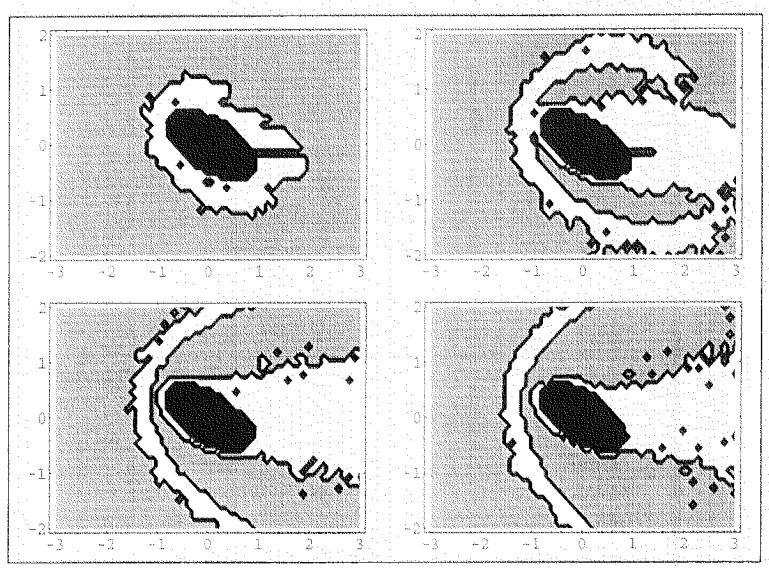

Figure 4: The domain decomposition of Boltzmann and Euler equations. In the upper half the domain decomposition is shown at time steps 10 (left) and 25 (right) and in the lower half for time steps 50 (left) and 100(right). White and gray domains represent the Boltzmann and Euler ones respectively

The white part indicates the Boltzmann domain and the gray one is that of Euler. This domain decomposition is similar to those obtained in [18], [19].

Finally, we compute the eigenvalues of the matrix V in (57). This is obtained from some transformation. Clearly, the matrices M from (38) and V from (57) do not share the same eigenvalues. But, the order of V is smaller than that of M.

In Figure 5 we have plotted, in a steady state, the three eigenvalues of the matrix V on the middle row of the computational domain. We see that one eigenvalue of V is also negative in the shock region. The other two eigenvalues are positive but have large deviations from unity in the non-equilibrium regions.

We again compute the three normalized invariants of the matrix V. Let $\lambda_1, \lambda_2, \lambda_3$ be three eigenvalues of the matrix V. These eigenvalues are close

to unity if the distribution function f is close to a local Maxwellian, then the following relations hold:

$$\frac{1}{3}(\lambda_1 + \lambda_2 + \lambda_3) = 1 \tag{64}$$

$$\frac{1}{3}(\lambda_1\lambda_2 + \lambda_2\lambda_3 + \lambda_1\lambda_3) = 1 \tag{65}$$

$$\lambda_1 \cdot \lambda_2 \cdot \lambda_3 = 1. \tag{66}$$

In Figure 6 we have drawn the three normalized invariants (64) - (66).

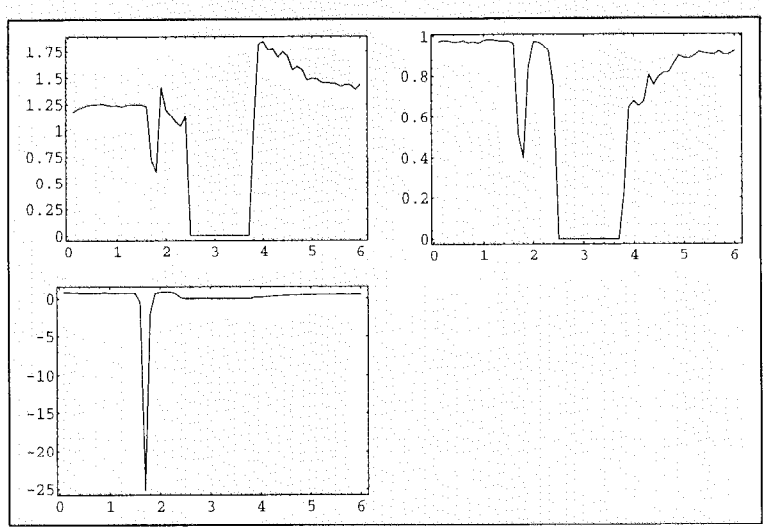

Figure 5: Three eigenvalues of the matrix V

As a criterion for a local thermal equilibrium we consider the invariant (66). We assume that if this invariant lies between 0.85 and 1.15, the cells are the Euler ones, otherwise they are Boltzmann ones. The domain decomposition obtained from this assumption, is similar to the Figure 4.

One can also use the other two invariants (64) and (65), with other tuning

parameters. They also give similar results.

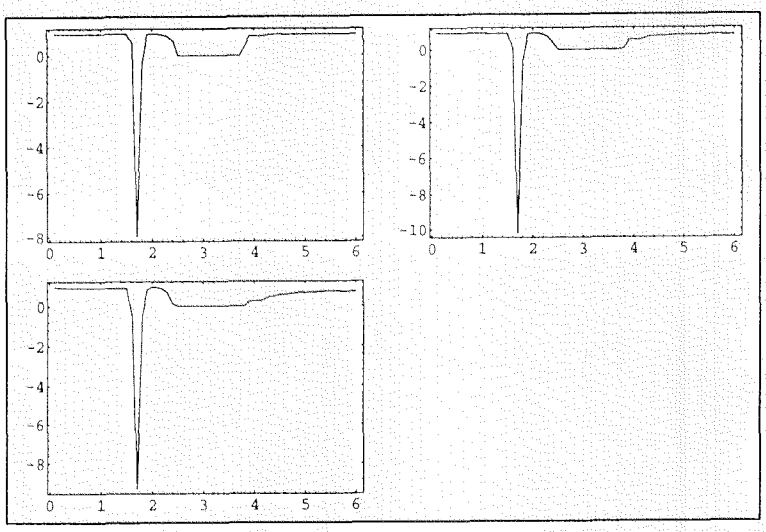

Figure 6: Three invariants of the matrix V

Our reference solutions are those obtained from the pure Boltzmann code. Therefore, we compare the solutions obtained from the coupling code with those from the pure Boltzmann one. We have plotted in Figure 7 the contour plots of the density, temperature and the Mach number from both codes. Clearly, the results performed both codes are very close to each other.

The the above test case the CPU times for the Coupling and pure Boltzmann codes are same. The computational efforts for the coupling code is much lower in comparison to the pure Boltzmann code, if one considers the adaptive solution techniques [20]. For the small mean free path one has to consider the cell size for the Boltzmann solver is of order of the mean free path. But for the Euler solver, it is not necessary to have the grid size of order of that kind.

Acknowledgements
The Author is grateful to Prof. H. Neunzert and Prof. C. D. Levermore for interesting discussions and information. The author further thankfully acknowledges the financial support provided by DAAD(German Academic Exchange Service).

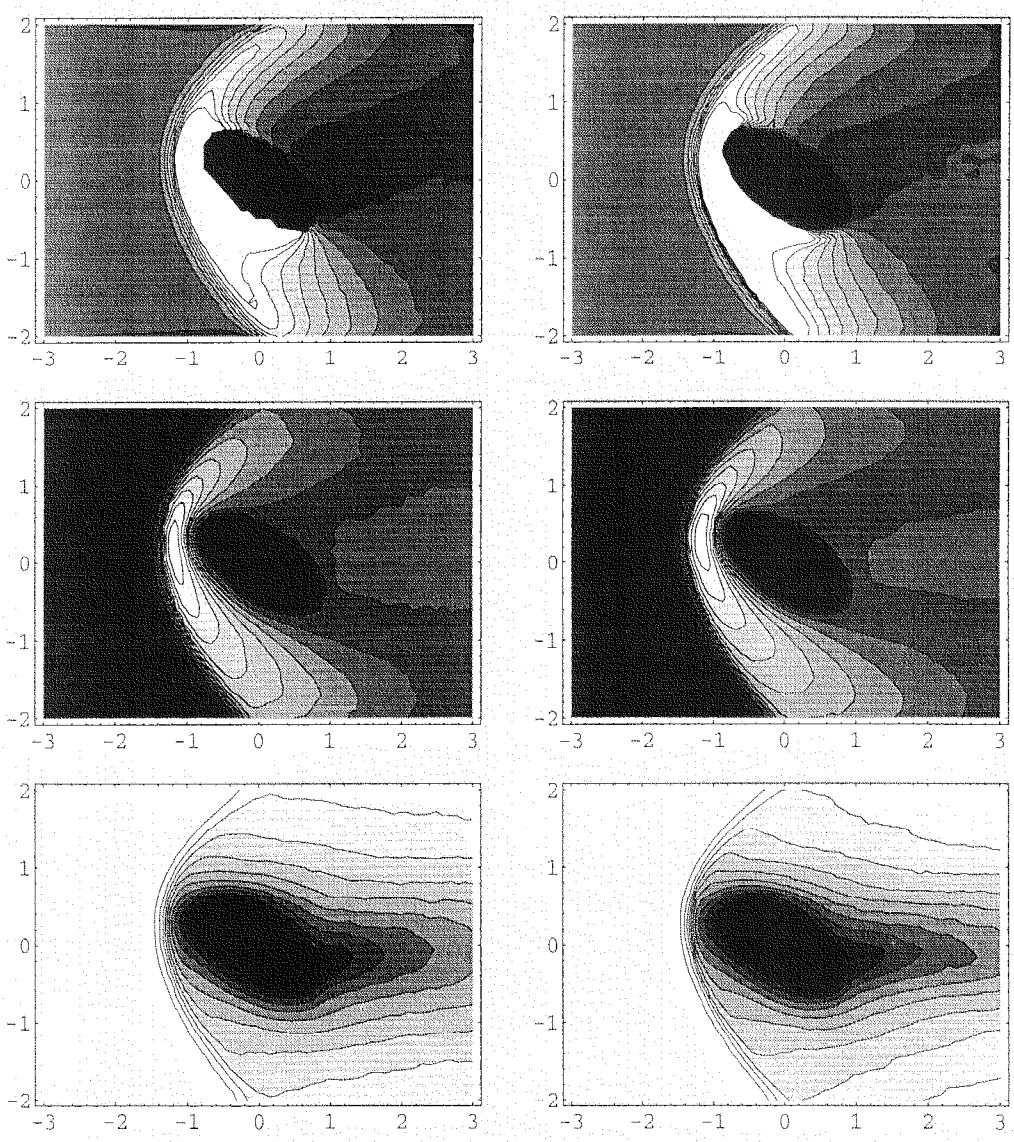

Figure 7: Contour plots of density (row 1), temperature (row 2) and Mach number. Pictures on the left are from the pure Boltzmann code and pictures on the right are from the coupling code

References

[1] H. Babovsky. *On a simulation scheme for the Boltzmann equation*, Math. Methods. Appl. Sci. **8**, 223 (1986).

[2] H. Babovsky. *A Convergence proof for Nanbu's Boltzmann simulation scheme*, Eur. J. Mech., **8**, 41 (1989).

[3] G. A. Bird. *Molecular Gas Dynamics*, (Clarendon Press, Oxford, 1976).

[4] J. F. Bourgat, P. Le Tallec, F. Mallinger, B. Perthame and Y. Qin. *Coupling Boltzmann and Euler Equations with overlapping*, Report INRIA 1991 (unpublished).

[5] J. F. Bourgat, P. Le Tallec and M. D. Tidriri. *Coupling Boltzmann and Navier-Stokes equations by friction*, J. Comp. Phys. **127**, 227 (1996).

[6] R. Caflish. The fluid dynamic limit of the nonlinear Boltzmann equation, CPAM, **33**, 651 (1980).

[7] C. Cercignani, R. Illner, M. Pulvirenti. *The Mathematical Thoery of Dilute Gases*, (Springer-Verlag New York, Berlin, Heidelberg 1994).

[8] F. Coron, B. Perthame. *Numerical Passage from Kinetic to Fluid Equations*, SIAM J. Numer. Anal., **28**(1), 26 (February 1991).

[9] S. M. Deshpande. *A second Order Accurate Kinetic Theory based Method for Inviscid Compressible Flows*, Tech. Paper 2613, NASA-Langley Research Center, Hampton, VA, 1986.

[10] E Godlewski and P. -A. Raviart. *Numerical Approximation of Hyperbolic System of Conservation Laws*, (Springer, 1995).

[11] S. Kaniel. *A Kinetic Model for the Compressible Flow Equations*, Indiana University Mathematics Journal, **37**(3), 537 (1988).

[12] A. Klar. *Domain Decomposition for Kinetic problems with nonequilibrium states*, Eur. J. Mech./B Fluids, **15**, 203 (1996).

[13] D. Levermore, William J. Morokoff, B. T. Nagida. *Moment realizability and the validity of the Navier-Stokes Equations for Rarefied Gas Dynamics*, preprint 1995.

[14] A. Lukschin, H. Neunzert, J. Struckmeier. *Coupling of Navier-Stokes and Boltzmann Regions*, Final Report for Project DPH 6473/91, Department of Mathematics, University of Kaiserslautern, 1992 (unpublished).

[15] H. Neunzert and J. Struckmeier. *Particle Methods for the Boltzmann Equation*, Acta Numerica, page 417 (Cambridge, 1995).

[16] J. Schneider. *Direct Coupling of Fluid and Kinetic Equations*, AGTM preprint No. 126, University of Kaiserslautern, 1995 (unpublished).

[17] J. Struckmeier and K. Steiner. *A comparison of simulation methods for rarefied gas flows*, Phys. Fluids, **7**, 11 (1995).

[18] S. Tiwari and S. Rjasanow. *Sobolev Norm as a criterion of local thermal equilibrium*, to appear in Eur. J. Mech. B/Fluids.

[19] S. Tiwari *Domain decomposition in particle methods for thr Boltzmann and Euler equations*, PhD Thesis, University of Kaiserslautern, 1998.

[20] S. Tiwari and A. Klar. *An Adaptive Domain Decomposition Procedure for the Boltzmann and Euler Equations*, preprint, 1997.